Title: Influence of aluminium alloy type on dissimilar friction stir lap welding of aluminium to copper

Author: I. Galvão D. Verdera D. Gesto A. Loureiro D.M. Rodrigues

PII: S0924-0136(13)00160-X
DOI: http://dx.doi.org/doi:10.1016/j.jmatprotec.2013.05.004
Reference: PROTEC 13686

To appear in: *Journal of Materials Processing Technology*

Received date: 11-2-2013
Revised date: 5-5-2013
Accepted date: 7-5-2013

Please cite this article as: Galvão, I., Verdera, D., Gesto, D., Loureiro, A., Rodrigues, D.M., Influence of aluminium alloy type on dissimilar friction stir lap welding of aluminium to copper, *Journal of Materials Processing Technology* (2013), http://dx.doi.org/10.1016/j.jmatprotec.2013.05.004

INFLUENCE OF ALUMINIUM ALLOY TYPE ON DISSIMILAR FRICTION STIR LAP WELDING OF ALUMINIUM TO COPPER

I. Galvão[1], D. Verdera[2], D. Gesto[2], A. Loureiro[1], D.M. Rodrigues[1,*]

1 - CEMUC, University of Coimbra, Rua Luís Reis Santos, 3030-788 Coimbra, Portugal

2 - AIMEN, Relva 27A Torneiros, 36410 Porriño, Spain

* dulce.rodrigues@dem.uc.pt, tel. + (351) 239 790 700, fax. + (351) 239 790 701

ABSTRACT

A Heat-treatable (AA 6082) and a non-heat treatable (AA 5083) aluminium alloys were friction stir lap welded to copper using the same welding parameters. Macro and microscopic analysis of the welds enabled to detect important differences in welding results, according to the aluminium alloy type. Whereas important internal defects, resulting from ineffective materials mixing, were detected for the AA 5083/copper welds, a relatively uniform material mixing was detected in the AA 6082/copper welds. Micro-hardness testing and XRD analysis also showed important differences in microstructural evolution for both types of welds. TEM and EBSD-based study of the AA 5083/copper welds revealed the formation of submicron-sized microstructures in the stirred aluminium region, for which untypically high hardness values were registered.

Keywords: Friction stir lap welding; AA 6082/copper; AA 5083/copper; Microstructure

INTRODUCTION

Despite the large number of potential industrial applications of aluminium/copper (Al/Cu) hybrid components, in practice, the use of this metallic couple remains limited. The different physical and mechanical properties of both metals, as well as its chemical affinity at temperatures higher than 120 ºC, which often results in extensive brittle intermetallic phases formation during welding, make the joining of these two materials very difficult. Although some success in Al/Cu joining has already been achieved by friction and explosion welding, strong restrictions in the thickness of the welded plates and joint geometry limit the wider application of these processes.

Friction stir welding (FSW), a welding technology, which, although has initially been developed for Al-alloys, soon spread to many other materials and materials combinations, renewed the hope of joining aluminium to copper for a large range of plate thicknesses and varied joint geometries (Çam, 2011). In this technology, a stirring tool composed of suitable designed shoulder and pin, which protrudes from the base of the tool shoulder, is pressed against plates to be welded and moves along them. The heat caused by the friction between the tool and the workpiece results in intense local heating that does not melt the plates to be joined, but severely deforms the material around the tool. The production of welds by plastic deformation, at temperatures below the melting temperature of the base materials, is viewed as an interesting way for reducing the formation of brittle intermetallic phases during Al/Cu welding and, consequently, cracking in the joints. Actually, several works have already addressed dissimilar friction stir welding of these materials, in both butt and lap joint configurations. However, Al/Cu friction stir butt welding has been much more explored than lap joining, for which, so far, only a small number of studies was conducted.

Elrefaey et al. (2004) were one of the first investigating the feasibility of lap joining of 2 mm-thick AA1100 H24 plates to 1 mm-thick copper plates. They found that the joint strength strongly depended on the penetration depth of the pin tip into the copper surface. The authors observed that the joints showed very weak fracture loads when the pin did not penetrate in the copper surface. On

the other hand, slight penetration of the pin tip into the copper surface increased the joint strength significantly. Although the level of bond strength was quite low, it exhibited a general tendency to increase with a rise in the rotation speed.

Some years later, Abdollah-Zadeh et al. (2008) and Saeid et al. (2010), in friction stir lap welding of 4 mm-thick AA 1060 to 3 mm-thick commercially pure copper, pointed out two factors affecting the welding results, i.e., the amount of brittle and hard intermetallic compounds and the "cold weld" condition. Whereas the welds produced under very high heat input conditions (high rotation speed and low traverse speed) presented formation of brittle intermetallic layers, in which strong micro-cracking takes place, the welds carried out under low heat input conditions (low rotation speed and high traverse speed) displayed incompletely welded interfaces. According to the authors, the optimum welding results should be achieved by adjusting rotational and traverse speed values. In 2011, Xue et al. (2011) reported the beneficial effect of using a large pin diameter for friction sir welding AA 1060 aluminium alloy to commercially pure copper plates, both of 3 mm-thick. According to the authors, a larger diameter pin gives rise to a larger bonding area, which inhibits more effectively the cracks propagation during mechanical testing, enhancing the bonding strength of the Al/Cu interface.

More recently, Akbari et al. (2012) analysed the effect of base materials positioning on friction stir lap welding of 2 mm-thick plates of AA 7070 aluminium alloy to commercially pure copper. Welds produced with the aluminium alloy located on the top of joint and the copper at the bottom, as well as welds carried out with the reverse base materials positioning, were studied by the authors. It was observed that, under similar welding conditions, the strength of the joints produced with the aluminium plate on the top was higher than that of the welds carried out with the reverse materials positioning. According to Akbari et al. (2012), the influence of the base materials positioning on the mechanical properties of the joints is closely related with the way how it affects the heat input during welding. Effectively, the authors concluded that the higher strength of the

welds produced with the aluminium plate on the top of the joint is mainly influenced by the higher peak temperatures reached during welding with this plates' positioning.

In the same year, Firouzdor and Kou (2012) compared the results of AA 6061/commercially pure copper friction stir lap welding carried out by using two different welding procedures, which were called "conventional" and "modified" friction stir lap welding. In conventional welding, the 1.6 mm-thick AA 6061 aluminium alloy plate was placed at the top of the lap joint and the copper plate, with the same thickness, was placed at the bottom. On the other hand, in modified lap welding, the 1.6 mm-thick plates were positioned in the reverse way, i.e., the copper plate was placed at the top and the aluminium plate at the bottom. Furthermore, a smaller AA 6061 aluminium alloy plate was butt welded to the copper at the top of the joint, with a slight pin penetration into the bottom sheet. In butt welding, the pin was shifted into aluminium plate, which was positioned at the advancing side of the tool. As a result of their study, the authors found that modified lap FSW significantly improved the quality of the Al/Cu friction stir lap welds. In fact, for specific values of rotation and traverse speed, the joint strength and the ductility of the "modified" welds was about twice and five to nine times higher, respectively, than those of the "conventional welds". Firouzdor and Kou (2012) also observed that voids were no longer present along the Al–Cu interface as in conventional lap welds, which shifted the location of fracture in tensile testing from along the interface to through Cu.

This year, Bisadi et al. (2013), in friction stir lap welding of 2.5 mm-thick AA 5083 to 3 mm-thick commercially pure copper sheets, claimed, in good agreement with Abdollah-Zadeh et al. (2008) and Saeid et al. (2010), that extreme welding temperatures give rise to defective joints. The authors observed channel-like defects near the sheets interface, for very low temperatures, and cavities at the interface of stirred aluminium particles and the copper, for high welding temperatures. According to the authors, high welding temperatures lead to higher aluminium diffusion to the copper sheet, which makes that aluminium particles are forced into the copper sheet and, after quenching, some cavities are formed at the interface of the particles and the copper

matrix. Besides the high temperatures, the different melting temperatures and contraction coefficients of both materials are pointed by the authors as the main factors on the basis of this type of defect. It was also reported that, for the range of welds tested, the hardness values of the stirred aluminium alloy were considerably lower than that of the aluminium base material, contrary to the stirred copper hardness, which was in over-match relative to the base material.

Excepting the works conducted by Akbari et al. (2012) and Firouzdor and Kou (2012), in all other studies presented above, the aluminium plates were positioned at the top of the Al/Cu lap joint and the copper plates at the bottom. Aluminium to copper friction stir lap welding with reverse plates positioning, enabling the joining of very thin copper plates to thicker aluminium plates remains deeply unexplored. This joint configuration, which, for example, enables copper cladding over small areas, has high technical and economic interest. Furthermore, most of the reported works were focused on welding of copper to commercially pure aluminium (1xxx aluminium series). Effectively, so far, only few works have already addressed friction stir lap welding of copper and aluminium alloys of other series with high industrial applicability, such as 6xxx and 5xxx aluminium series. In this context, dissimilar friction stir welding of 1 mm-thick copper-DHP plates to 6 mm-thick AA 5083-H111 and AA 6082-T6 aluminium alloys plates, with the copper plate located at the top of the joint, was carried out in present work. The influence of the base materials intrinsic properties on Al/Cu friction stir weldability, which has never been investigated, was studied by performing a deep structural and mechanical characterization of the welds.

EXPERIMENTAL PROCEDURE

Copper-DHP (R240) was friction stir lap welded to two different aluminium alloys, the heat treatable AA 6082-T6 and the non-heat treatable AA 5083-H111 alloy, in a MTS I-Stir PDS equipment. As illustrated in Figure 1, the 1 mm-thick copper-DHP plates were placed at the top of 6

mm-thick plates of each aluminium alloy, being clamped against it. Welding was carried out with a tool composed of a 9.5 mm-diameter conical shoulder, with an 8º cavity, and a 3 mm-diameter and 1 mm-long cylindrical probe, which is schematically represented in Figure 2. In order to study the effect of the aluminium alloy type on welding results, all welds were conducted using the same welding parameters, namely, rotational and traverse speeds of 600 rev.min^{-1} and 50 mm.min^{-1}, respectively, tool tilt angle of 0º and tool axial load of 4.5 kN. In this way, the nomenclature adopted in the text for labelling the different welds will identify the only variable welding condition, i.e., the aluminium alloy. So, copper-DHP/AA 5083-H111 and copper-DHP/AA 6082-T6 welds will be identified by the acronyms W5 and W6, respectively.

After welding, a qualitative macroscopic inspection of the weld surfaces was performed by means of visual inspection. Transverse cross-sectioning of the welds was performed for metallographic analysis. The samples were prepared according to standard metallographic practice and differentially etched in order to enable the analysis of the microstructural transformation induced by welding. Metallographic analysis was performed using optical microscopy, in a ZEISS 100 HD equipment. The microstructure of some selected welds was also analysed by transmission electron microscopy (TEM) and electron backscatter diffraction (EBSD) in a FEI Tecnai G^2 S-Twin and a FEI Quanta 400FEG ESEM/EDAX Genesis X4M microscopes, respectively. Microhardness measurements were performed using a Shimadzu Microhardness Tester, with 200 g load and 15 s holding time. Micro X-ray diffraction and electron probe micro analysis (EPMA) were performed in the cross-section of the welds using a PANalytical X´Pert PRO micro-diffractometer and a Cameca Camebax SX50 apparatus, respectively.

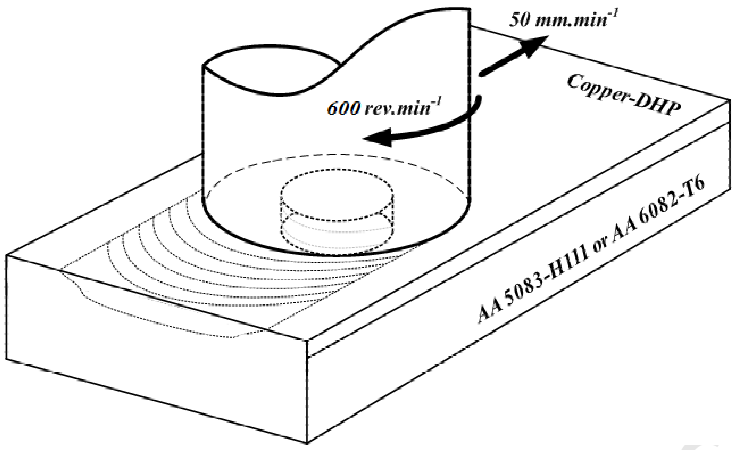

Figure 1 - Schematic representation of Al/Cu friction stir welding.

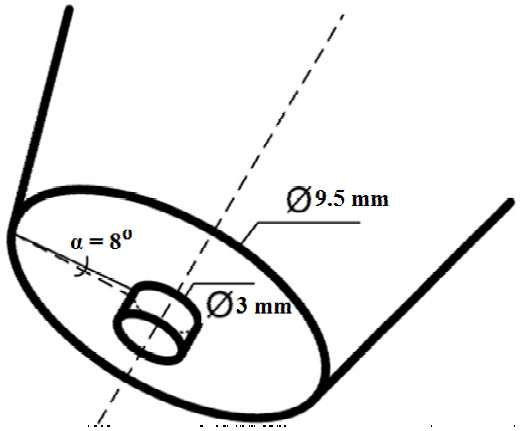

Figure 2 - Friction stir welding tool.

RESULTS

Welds structure and morphology

Images of the surfaces, cross-section macrographs and micrographs registered in some selected cross-section areas of W5 and W6 welds are illustrated in Figures 3 and 4, respectively. Significant

differences in surface finishing can be observed by comparing the surface photographs in Figures 3.a and 4.a. In fact, whereas the W5 weld presents a very smooth surface composed of regular and well-defined striations, similar to those obtained in similar copper friction stir welding by Galvão et al. (2013), signs of significant tool submerging and formation of massive flash are observed at the surface of the W6 weld. It is important to stress that, although both welds have been carried out under the same welding conditions, the W6 weld surface presents defects usually associated to excessive heat input during friction stir welding. This result is in good agreement with Leitão et al. (2011), who studied the influence of base materials properties on defect formation during AA 5083 and AA6082 aluminium alloys FSW.

Comparing the cross-section macrographs of both welds, displayed in Figures 3.b and 4.b, for cooper etching, and in Figures 3.c and 4.c, for aluminium etching, important differences in the structure and morphology of the bonding area, where the top and bottom materials interact, can also be observed. Figures 3.b and c, which display the cross-section of the W5 weld, show that the Al-Cu interaction zone of this weld is restricted to the pin influence zone, where a very fine recrystallized grain structure is discernible for both base materials. Very small evidence of material stirred by the shoulder can be observed at the top of the weld in Figure 3.b, indicating that the shoulder influence zone was restricted to the top surface of the copper plate. The totally inefficient mixing, between aluminium and copper, gave rise to a large discontinuity between both base materials, preventing the effective joining of the plates. Actually, according to Figure 3, coupling between the two materials only occurred at the advancing side of the tool where the aluminium was pushed upward, into the copper plate.

The cross-section macrographs of the W6 weld are shown in Figures 4.b and c. From the pictures, it can be concluded that the Cu/Al interaction volume for the W6 weld is significantly larger than that observed for the W5 weld. The picture in Figure 4.b also shows the presence of a well-defined shoulder influenced zone, encompassing the entire copper plate's thickness. This is also enhanced in Figure 4.d where deformed copper grains are discernible across the entire plate

thickness. This enables to conclude that, under the same axial loading conditions, a larger amount of copper was dragged by the shoulder for the W6 weld than for the W5 weld. In good agreement with this, as illustrated in Figure 4.e, strong base materials interaction took place during W6 welding, resulting in the formation of mixing structures with morphology similar to those observed by Galvão et al. (2011) and Galvão et al. (2012) in Al-Cu friction stir butt welding. In fact, a complex mixing structure composed of copper and aluminium intercalated with lamellae of material morphologically different of both base materials, which, according to these authors, have intermetallic-rich phase composition, is discernible in Figure 4.e.

However, in spite of a more efficient base materials mixing than in W5 welding, which points to a stronger interaction between both base materials, some internal defects were also observed for the W6 weld, specifically, micro-discontinuities embedded in the mixing structures of Figure 4.e. It is important to stress that these defects, besides presenting different morphology, are significantly smaller than those observed for the W5 weld. Non-uniform base materials mixing, which should result in the appearance of small discontinuities, as well as the strong brittleness of new Al-Cu phases, formed during welding, should have some influence on material flow, giving rise to this type of defects. According to Abdollah-Zadeh et al. (2008) and Saeid et al. (2010), cracking incidence in intermetallic-rich zones is one of the main causes for the premature failure of dissimilar Al-Cu friction stir welds. This way, it can be concluded that stronger base materials mixing during dissimilar Al-Cu welding does not necessarily mean sound joining.

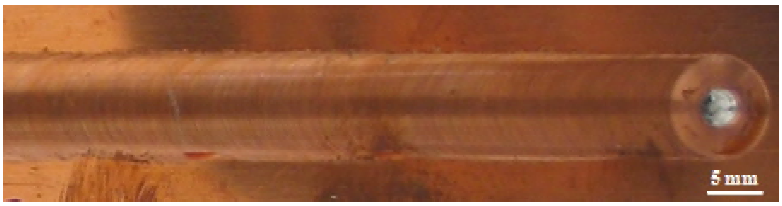

(a)

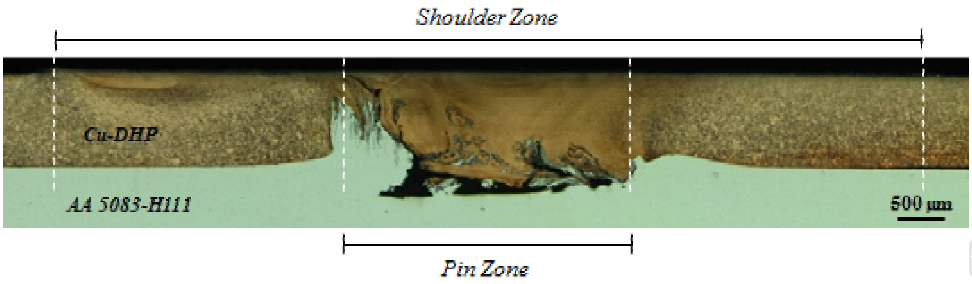

(b)

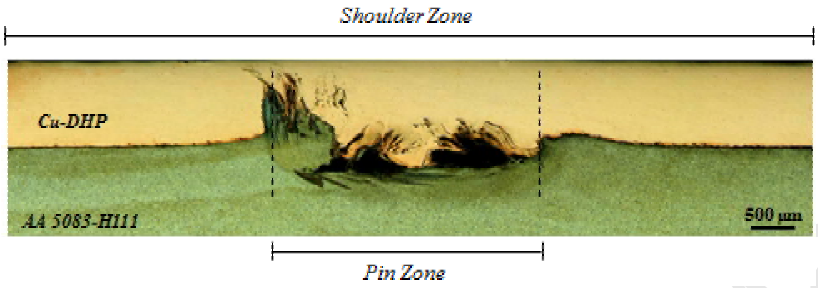

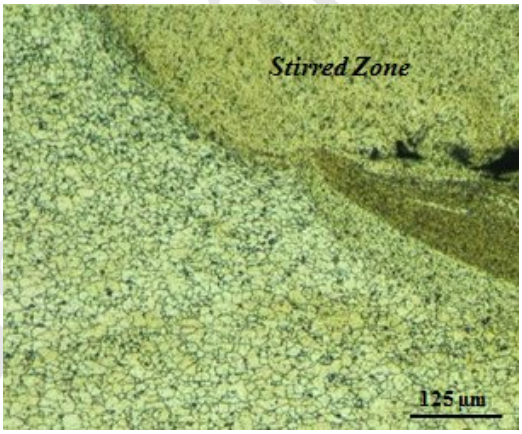

(c) (d)

Figure 3 - Surface photograph (a); copper (b) and aluminium (c) etched cross-section macrographs and micrograph of the aluminium stirred zone (d) of the W5 weld.

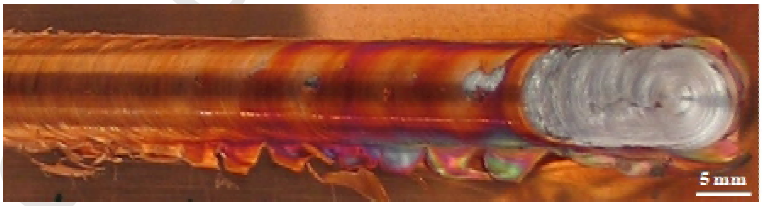

(a)

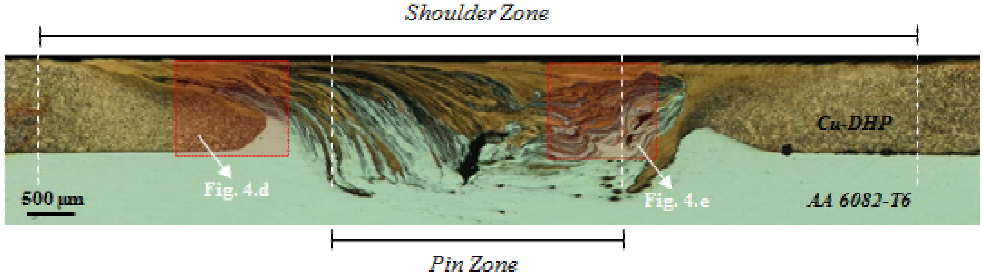

(b)

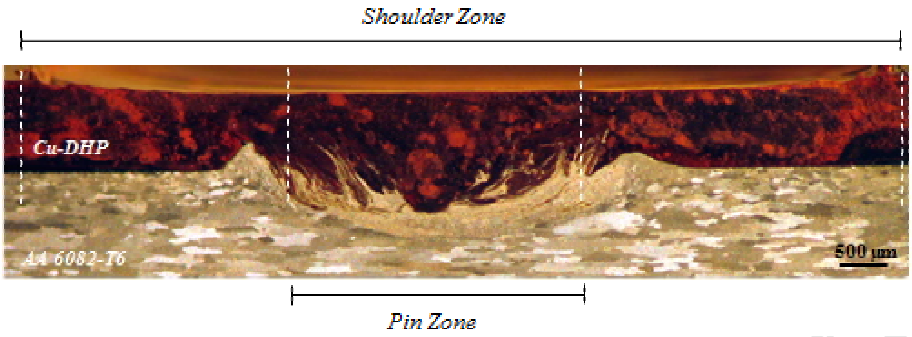

(c)

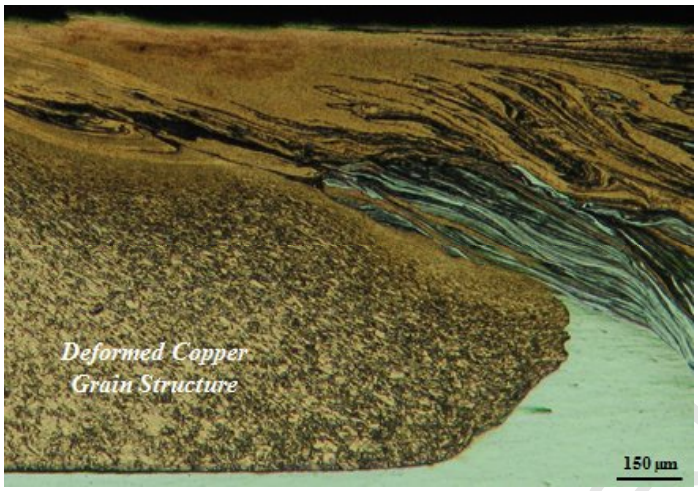

(d)

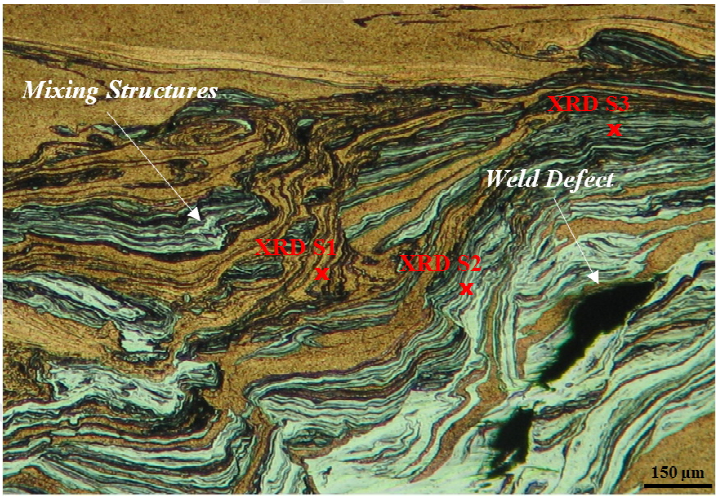

(e)

Figure 4 - Surface photograph (a); copper (b) and aluminium (c) etched cross-section macrographs and micrographs of the under shoulder copper structure (d) and of the mixing structures (e) of the W6 weld.

Figure 5 shows hardness profiles registered across the transverse sections of W5 (Figure 5.a) and W6 (Figure 5.b) welds. Each graph shows the results of hardness measurements performed along horizontal planes located in the top (copper) and bottom (aluminium) plates, as illustrated by the horizontal lines plotted in the cross-section pictures included in the figure. The average hardness of the base materials is also indicated in the graphs by short lines, located at each side of the hardness profiles. According to the figures, whereas for the W5 weld an important increase in hardness was registered for both the AA 5083 (W5 Al) and copper (W5 Cu) stirred zones, for the

W6 weld, the hardness increase was restricted to the upper copper layer (W6 Cu), being registered a smooth hardness decrease in the stirred AA 6082 aluminium alloy (W6 Al). For the W5 weld, further hardness measurements, performed closer to the stirred Al-Cu interface (□ 125 µm from the bonding discontinuity), as illustrated in Figure 6, allowed observing the existence of an important hardness gradient inside the AA 5083 stirred volume. The hardness values measured in this zone, which range from 158 $HV_{0.2}$ to 215 $HV_{0.2}$, are higher than those of the W5 Al hardness profile in Figure 5.a and much higher than the hardness values reported by Hirata et al. (2007), El-Danaf et al. (2010) and Tronci et al. (2011), in similar AA 5083 friction stir welding/processing, and by Bisadi et al. (2013), in dissimilar AA 5083/copper FSW.

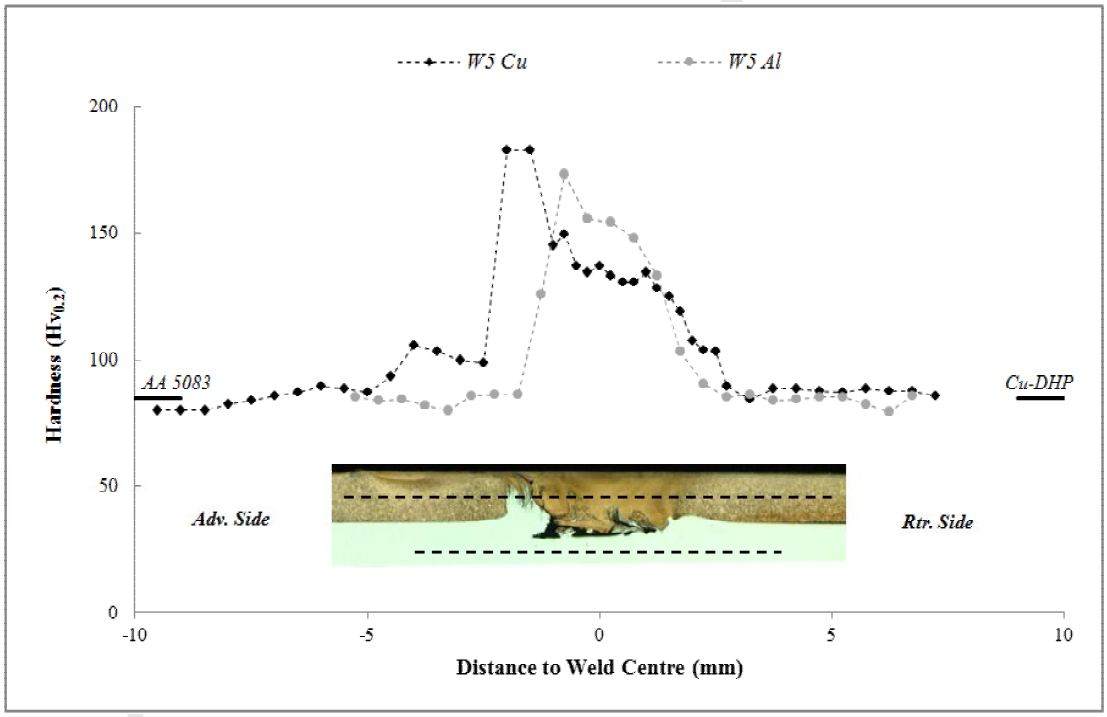

(a)

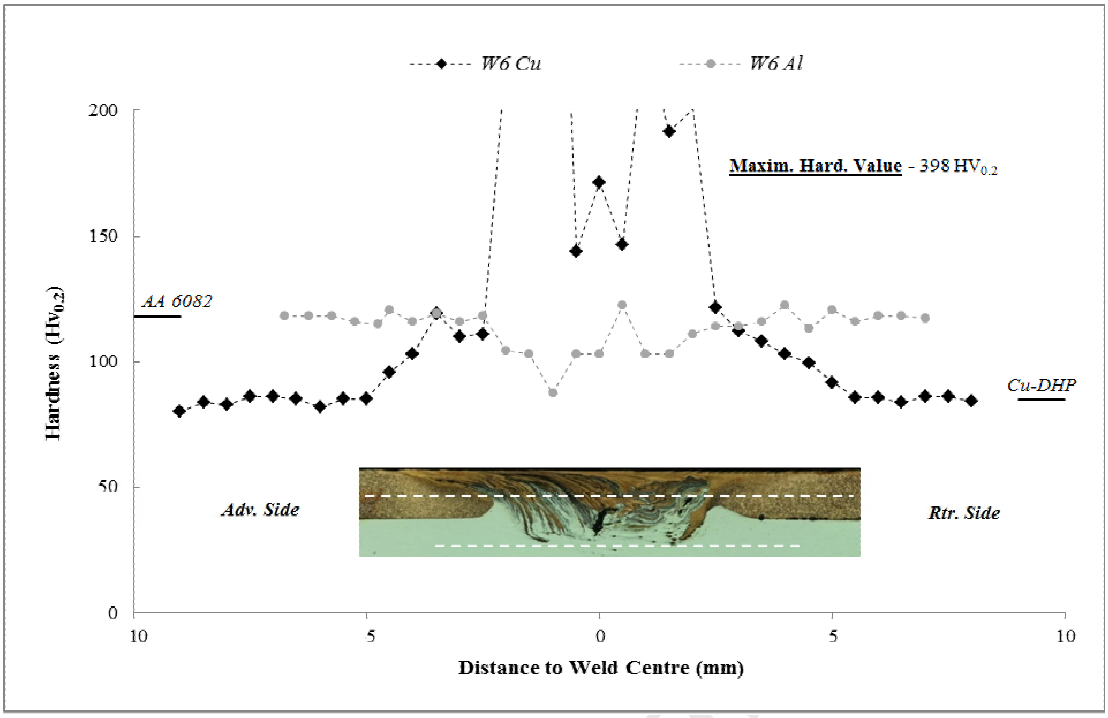

(b)

Figure 5 - Hardness profiles registered across the transverse cross-section of the W5 (a) and W6 (b) welds.

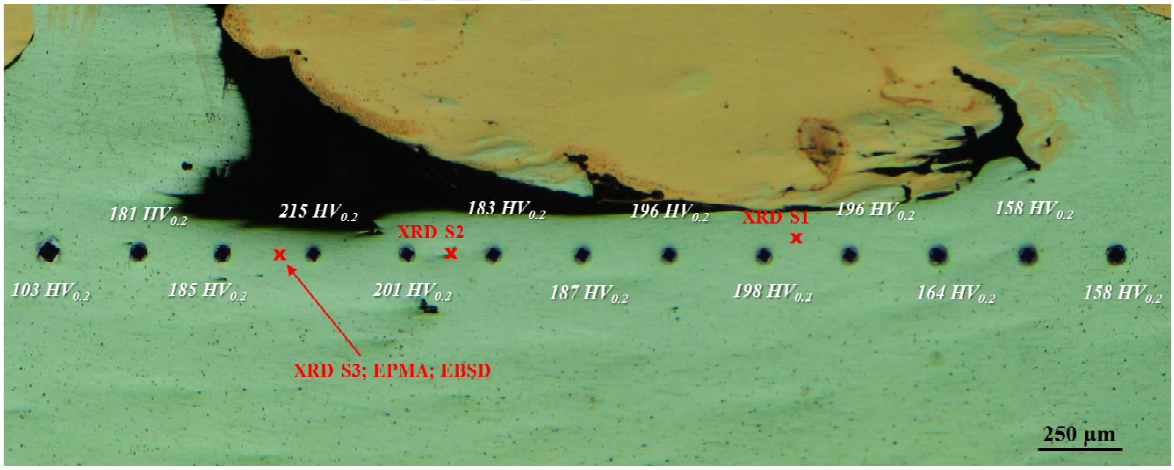

Figure 6 - Hardness values registered in the aluminium stirred region of the W5 weld, in the vicinity of the Al-Cu interface.

Two main factors can be related to the very important, and non-expectable, hardness increase inside the stirred volume of the W5 weld: one is the intense grain refinement which can be noticed inside the stirred volumes displayed in Figures 3.b to d, the other is the formation of new Al-Cu phases, either solid solution phases or intermetallic compounds, inside the stirred volume, as previously reported by Ouyang et al. (2006) and Galvão et al. (2011). The same phenomena should be associated with the hardness increase registered in the upper copper layer of the W6 weld. In opposition to this, the hardness decrease registered inside the AA 6082 stirred volume is undoubtedly related to the heat-treatable nature of this alloy. As well-documented in previous studies, such as in Svensson et al. (2000), the hardness of this material is determined by the size and dispersion of strengthening precipitates rather than by the grain size. The dissolution of strengthening phases in the stirred zone and coarsening of strengthening particles in the heat affected zone are the main causes for the hardness losses in this alloy.

In order to understand the sharp hardness increase inside the stirred volumes of the W5 and W6 welds, XRD analyses were accomplished enabling to determine the phase content in the highest hardness zones of both welds. For the W5 weld, the area analysed corresponded to the refined aluminium layer, in the vicinity of the Al-Cu interface (see S1, S2 and S3 points in Figure 6). For the W6 weld, the area analysed was located inside the stirred/mixing material region (see S1, S2 and S3 points in Figure 4e). The diffractograms obtained for the W5 and W6 welds are displayed in Figure 7. According to the diffractogram corresponding to the W5 weld (Figure 7.a), the only phase detected in the area analysed was f.c.c. Al. In order to complement the XRD results for the W5 weld, the elemental chemical composition of the refined aluminium layer was also investigated by performing electron probe microanalysis (see EPMA analysis zone in Figure 6). From Figure 8, where the results of this analysis are displayed, it can be concluded that only Al and small amounts of Mg and Mn, which are the main alloy elements of the AA 5083 alloy, were identified in this zone, which is in good agreement with the XRD results. In this way, it is possible to conclude that the formation of new Al-Cu intermetallic phases during welding is not on the basis of the strong

hardness increase (from 85 $HV_{0.2}$ to 215 $HV_{0.2}$) registered in the refined aluminium layer. On the other hand, for the W6 weld (Figure 7.b), for which intense material mixing inside the stirred volume can be observed in Figure 4, and very high hardness values were also registered (□ 400 $HV_{0.2}$), the XRD analysis enabled to identify the presence of important amounts of Cu_9Al_4 and small amounts of $CuAl_2$, which are responsible for the hardness increase.

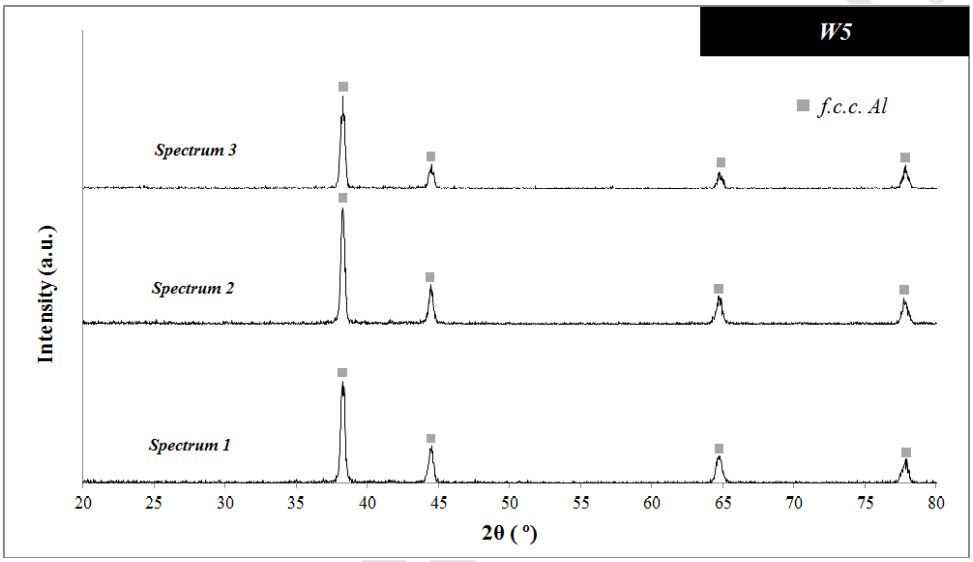

(a)

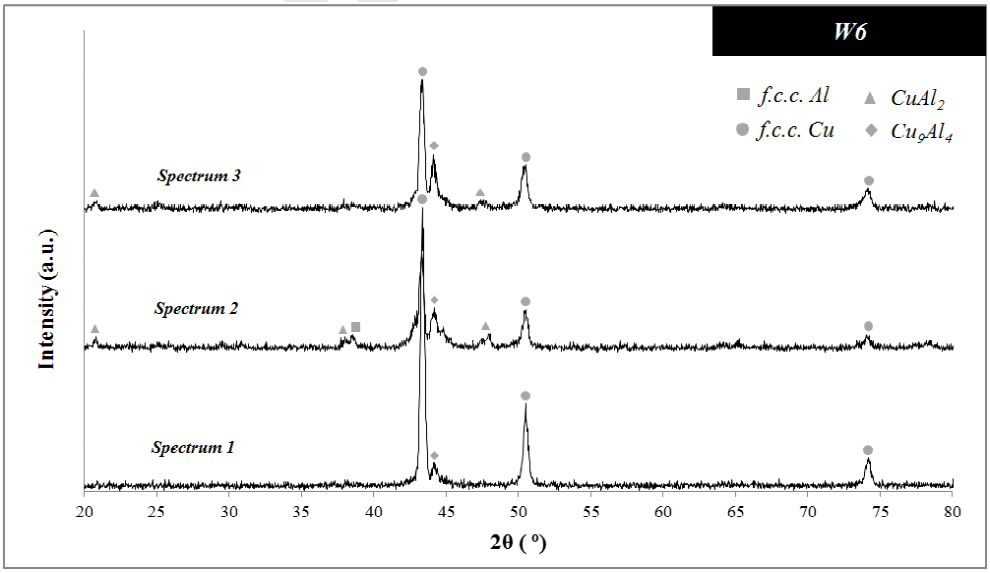

(b)

Figure 7 - Results of the XRD inspection carried out in the stirred zone of the W5 (a) and W6 (b) welds.

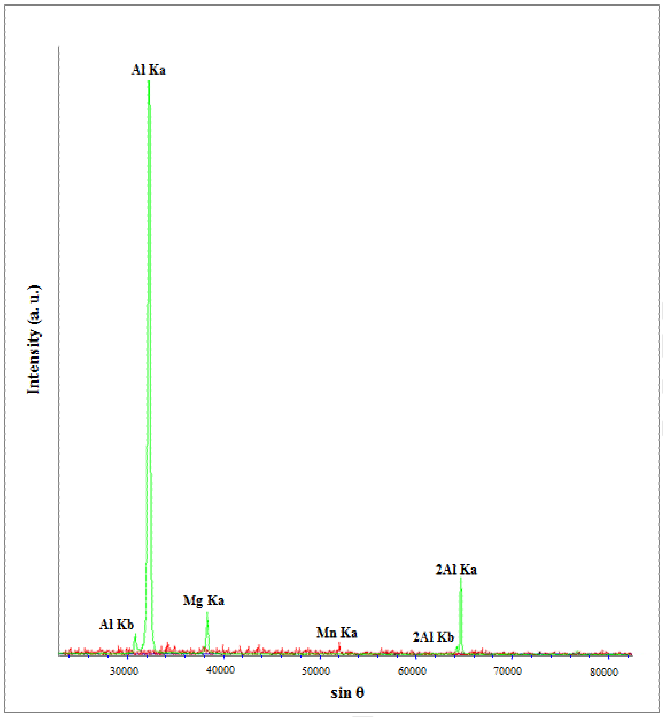

Figure 8 - Qualitative chemical analysis (EPMA) carried out in the stirred aluminium region of the W5 weld, in the vicinity of the Al-Cu interface.

DISCUSSION

Influence of the aluminium alloy type on the welding results

Since both weld types analysed in this work were carried out under the same welding conditions, a strong influence of aluminium alloys type on welding results has to be pointed. Actually, Leitão et al. (2012a) and Leitão et al. (2012b) have already addressed the influence of the markedly different mechanical behaviours of the AA 5083 and the AA 6082 aluminium alloys, at high temperature and strain rates, on the friction stir weldability of both alloys. According to these authors, whereas the

AA 6082 aluminium alloy experiences strong softening with plastic deformation at increasing temperatures, which is traduced by a strong decrease of the flow stresses of the material with plastic deformation, the AA 5083 alloy presents, at high temperatures, steady flow stress behaviour. As a result of this, under the same axial load during FSW, the higher thermal softening experienced by the AA 6082 alloy led to further submerging of the tool during welding, relative to the 5083 alloy, which resulted in the strong deepening and massive flash formation observed at the surface of the W6 weld (Figure 4.a). The higher tool submerging during AA 6082/copper-DHP welding also resulted in increased amounts of copper and aluminium being dragged by the shoulder and the pin, respectively, into the shear layer at each tool revolution. The strong pin-governed base materials mixing at the shear layer resulted in the formation of the mixing structures observed in the stirred zone of the W6 weld (Figure 4.e). As opposed to this, for the W5 weld, the significantly smaller volume of copper dragged by the tool, at each revolution, as well as the less efficient material dragging promoted by the pin in the AA 5083 alloy, prevented strong base materials interaction in the shear layer, which resulted in the formation of a discontinuous aluminium/copper interface in the stirred zone.

Microstructural evolution of the AA 5083 aluminium alloy during welding

Hardness values in the range of 200 $HV_{0.2}$ were registered in the refined aluminium region of the W5 weld. Taking into account that, according to Figures 7.a and 8, no Al-Cu phases were formed in that zone, this hardness increase may be considered surprisingly high. In order to understand this phenomenon, a deep TEM and EBSD-based microstructural study of the W5 weld was performed.

Results of the TEM analysis carried out in the stirred aluminium region of the W5 weld, where the hardness profile of Figure 5.a was registered, are illustrated in Figure 9.a. It can be observed that equiaxed submicron sized grains, with well-defined grain boundaries and low dislocations density, compose the microstructure of the stirred aluminium region. A histogram

representing the grain size distribution in this zone, plotted after performing hundreds of grain measurements over several TEM micrographs, is illustrated in Figure 9.b. The histogram shows an average grain size of 325 nm (± 90 nm), with most of the grains ranging between 150 nm and 450 nm. Previous metallographic analysis (Figure 3.d) enabled to determine an average grain size of 24 µm for the AA 5083 base material. The dynamic recrystallization taking place during FSW promoted the formation of an ultrafine-grained microstructure reported in Figure 9.

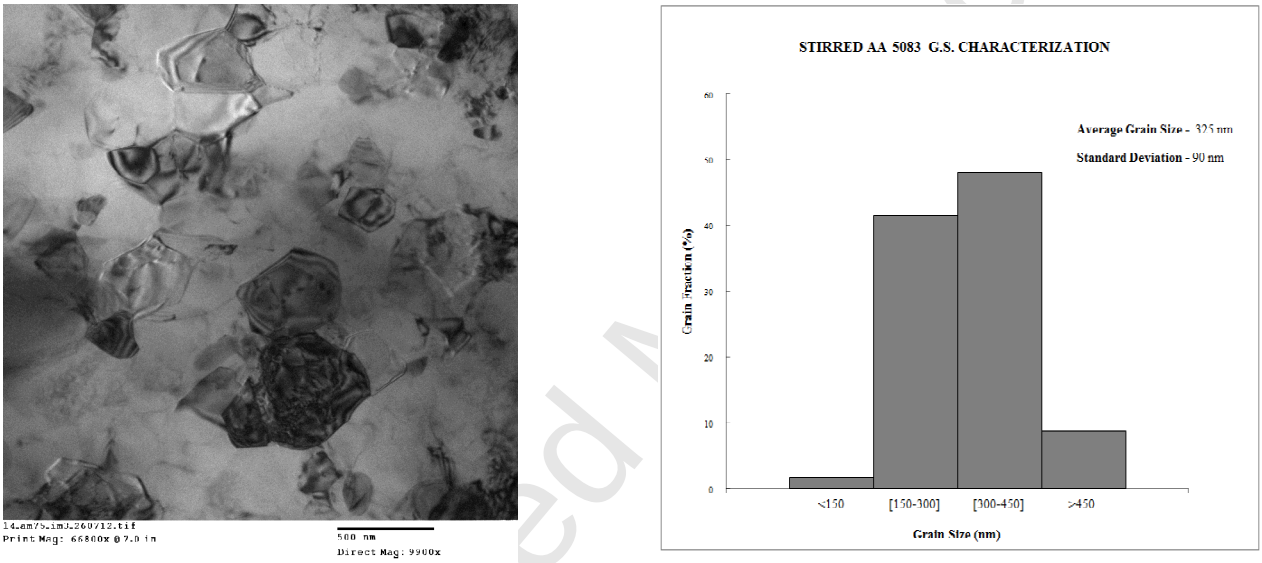

(a) (b)

Figure 9 - TEM micrograph registered in the stirred aluminium region of the W5 weld (a) and the grain size distribution in that zone (b).

The microstructure of the stirred aluminium layer was also studied by EBSD. Figure 10 illustrates EBSD patterns acquired in two different zones of the W5 weld, i.e., in the hard aluminium layer (Figure 10.a) and in the AA 5083 base material (Figure 10.b). Important differences can be observed by comparing both pictures. Effectively, contrary to that observed in the base material electron backscatter patterns (EBSPs), patterns overlapping can be observed in Figure 10.a, which corresponds to the analysis carried out in the stirred zone. According to Maitland and Sitzman (2007), the overlapping phenomenon takes place at grain boundaries when the electron

beam diameter is large enough to produce EBSPs from two grains simultaneously. Since the achievable resolution of EBSD for aluminium is typically □ 50 nm (Humphreys, 2004), patterns overlapping should indicate the presence of nano grains in the hard aluminium layer, with a grain size value in the range of the technique resolution. This value is about seven times lower than the TEM-based grain size. Effectively, the EBSD analysis was performed in an aluminium layer located in the vicinity of the Al/Cu discontinuity (see EBSD analysis zone in Figure 6), contrary to the TEM analysis, which was carried out at middle thickness of the aluminium stirred region. The grain size differences point to the existence of a grain size gradient across the thickness of the stirred zone, which is in good agreement with the hardness results shown in Figures 5.a and 6. The quite higher grain refinement and hardness increase in a very thin aluminium layer in the vicinity of the materials discontinuity are easily explained by the length of the tool pin used to produce the joints. In fact, during welding, the pin, whose length is 1 mm, i.e., the thickness of the top copper plate, performed tangentially to the superficial layer of the bottom aluminium plate, in which a stronger stirring action was promoted. As the rate of nucleation of new grains is proportional to the rate of plastic deformation, more nucleation points are formed and, consequently, less grain growth took place in this zone, giving rise to stronger grain refinement and hardness increase.

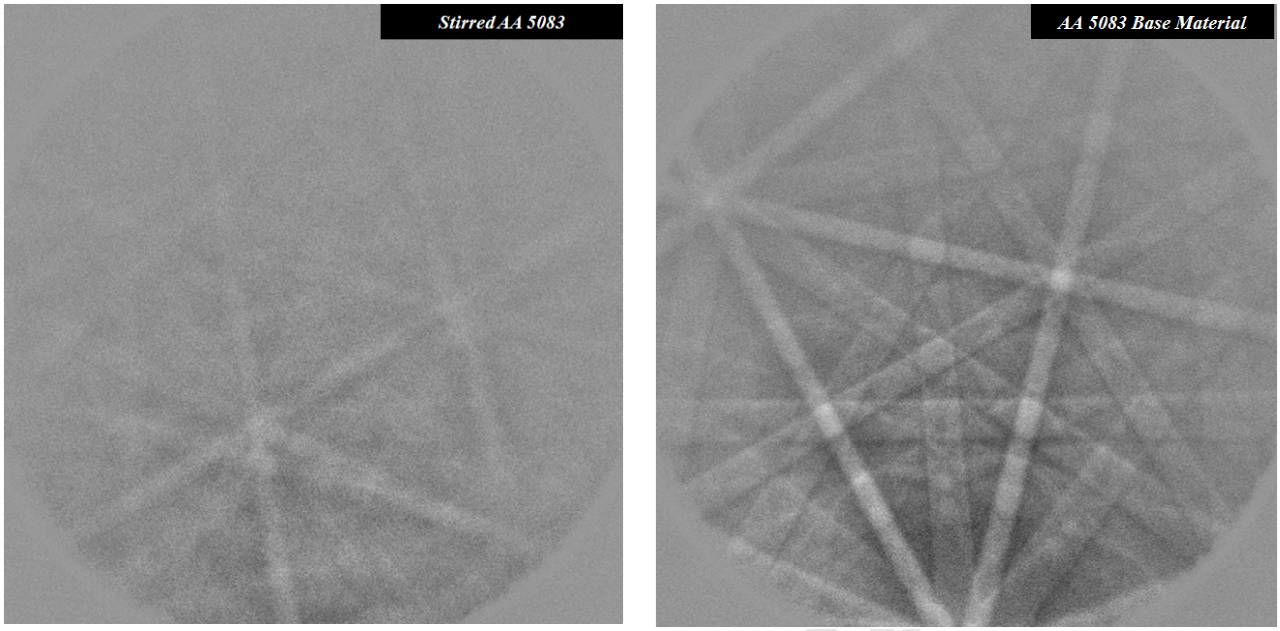

(a) (b)

Figure 10 - EBSD patterns acquired in the stirred aluminium layer of the W5 weld, in the vicinity of the Al-Cu interface (a), and in the AA 5083 base material (b).

The improvement of the AA 5083 aluminium alloy mechanical properties, by creating submicrometer or nanometric grain structures, has already been explored in several researches from other authors who used powder metallurgy and/or severe plastic deformation techniques (combined or not with friction stir processing) to obtain fine grained structures. Results from some of these studies are resumed in Figure 11, in which the AA 5083 hardness (HV) is plotted against the reciprocal of the square root of the grain size ($\mu m^{-1/2}$). The Hall-Petch equation was also fitted to the bibliographical results. Results from current work, namely, the average hardness values measured in the vicinity of the Al-Cu interface (190 $HV_{0.2}$) and some hundreds of micrometres below, across the W5 Al line displayed in Figure 5.a (135 $HV_{0.2}$), were also included in the graph. From the figure it can be observed that the grain size inside the AA5083 stirred volume of the W5 weld, obtained using elementary FSW procedures, is of the same magnitude of that obtained by other authors under other severe plastic deformation conditions.

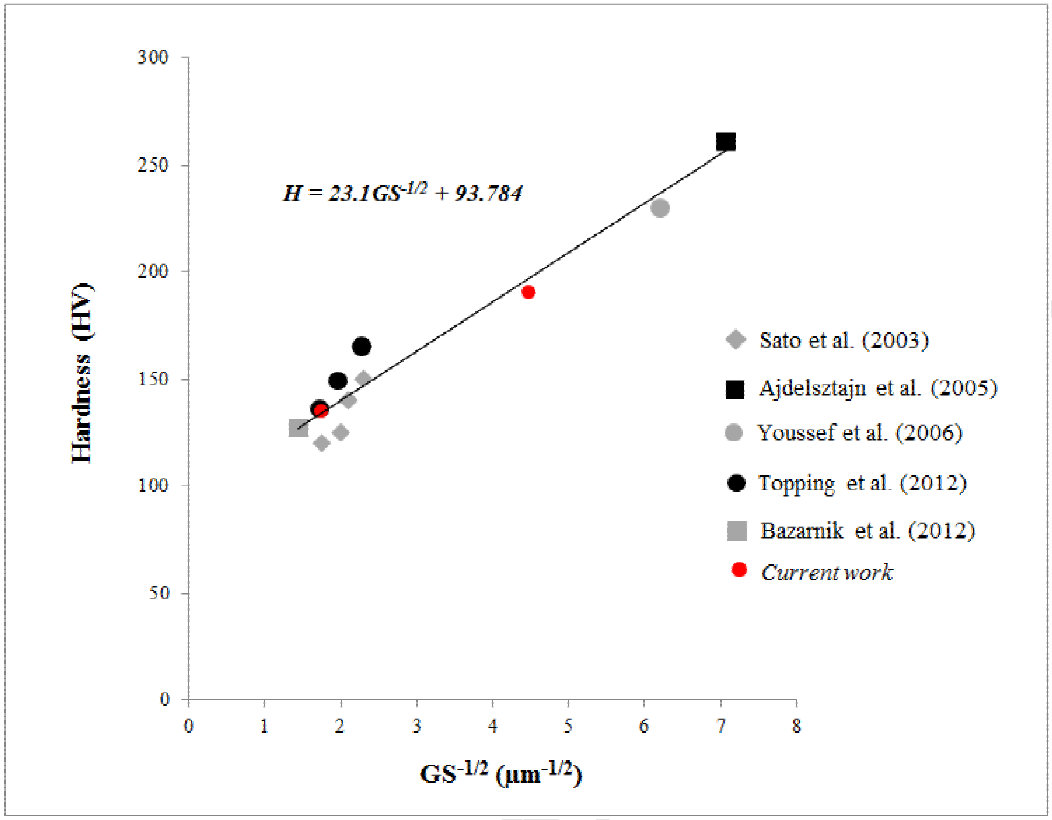

Figure 11 - Hall-Petch relationship for ultra-fine grained AA 5083 aluminium alloy.

The ultra-refined microstructure of the friction stir welded AA 5083 aluminium alloy, which resulted in an impressive hardness increase in the stirred zone of the W5 weld, is indicative of a very small thermal-activated grain growth after dynamic recrystallization. According to Cui et al. (2009), tool size and rotation/travel speed ratio have great influence on the grain size of the friction stir processed microstructures, which decreases for decreasing values of these parameters as a result of the lower heat input during welding. The rotation/traverse speed ratio used in present work is not significantly lower than that tested by Hirata et al. (2007), El-Danaf et al. (2010), Tronci et al. (2011) and Bisadi et al. (2013) in AA 5083 or AA 5083/copper-DHP friction stir welding/processing studies, for which significantly coarser and softer microstructures were achieved. However, the tool used to produce the welds is significantly smaller than the tools usually reported in most of these works. According to Ma and Mishra (2005), lower values of tool shoulder and pin reduce the thermal input significantly because the decrease in the contact area between the

tool and workpiece and the decrease in the linear surface velocity of the tool. This way, it can be concluded that the very small tool used in present work, although does not have allowed a suitable material flow during welding, which resulted in the formation of important defects at the Al-Cu interface, promoted an impressive hardness increase in the aluminium alloy due to the formation of ultra-refined microstructure in this material. This conclusion can be the starting point for future researches focused on the production of sound AA 5083/Cu-DHP friction stir lap welds with improved mechanical properties. Combining materials' mechanical enhancement obtained in this study with proper friction stir welding conditions, which can be achieved by studying a larger range of welding parameters, is an attractive challenge for future works. Specifically, the production of mechanically enhanced Al/Cu cladded components, which combine copper´s thermal and electrical properties with aluminium's low specific weight and cost, by performing parallel friction welding passes all along the workpiece surface is a very interesting topic to be investigated.

CONCLUSIONS

The influence of aluminium alloy properties on Al/Cu friction stir weldability was analysed in this study for a specific set of welding parameters. The following conclusions can be drawn:

- The different plastic properties of the AA 5083 and AA 6082 aluminium alloys, at high temperature and strain rates, have an important effect on the metallurgical and material flow phenomena taking place during Al/Cu welding and, consequently, on the final properties of the welds;
- Whereas the AA 5083/copper-DHP welds presented excellent surface finishing, but highly defective Al/Cu interfaces, without any signs of base materials interaction, the AA 6082/copper-DHP welds displayed poor surface properties, but strong base materials mixing in the stirred zone;

- For the AA 5083/copper-DHP welds, an impressive hardness increase was registered in the aluminium part of the weld due to the formation of an ultra-refined microstructure;
- The very small tool used in present work played a decisive role in the microstructural evolution of the AA 5083-H111 aluminium alloy during welding.

ACKNOWLEDGEMENTS

This research is sponsored by FEDER funds through the program COMPETE and by national funds through FCT, under the project PEst-C/EME/UI0285/2011.

REFERENCES

Abdollah-Zadeh, A., Saeid, T., Sazgari, B., 2008. Microstructural and mechanical properties of friction stir welded aluminum/copper lap joints. J. Alloys Compd. 460, 535-538.

Ajdelsztajn, L., Jodoin, B., Kim, G.E., Schoenung, J.M., 2005. Cold Spray Deposition Aluminum Alloys. Metall. Mater. Trans. A 36A, 657-666.

Akbari, M., Abdi Behnagh, R., Dadvand, A., 2012. Effect of materials position on friction stir lap welding of Al to Cu. Sci. Technol. Weld. Joining 17, 581-588.

Bazarnik, P., Lewandowska, M., Andrzejczuk, M., Kurzydlowski, K.J., 2012. The strength and thermal stability of Al–5Mg alloys nano-engineered using methods of metal forming. Mater. Sci. Eng. A 556, 134-139.

Bisadi, H., Tavakoli, A., Sangsaraki, M.T., Sangsaraki, K.T., 2013. The influences of rotational and welding speeds on microstructures and mechanical properties of friction stir welded Al5083 and commercially pure copper sheets lap joints. Mater. Des. 43, 80-88.

Çam, G., 2011. Friction stir welded structural materials: beyond Al-alloys. Int. Mater. Rev. 56, 1-48.

Cui, G.R., Ma, Z.Y., Li, S.X., 2009. The origin of non-uniform microstructure and its effects on the mechanical properties of a friction stir processed Al-Mg alloy. Acta Mater. 57, 5718-5729.

El-Danaf, E.A., El-Rayes, M.M., Soliman, M.S., 2010. Friction stir processing: An effective technique to refine grain structure and enhance ductility. Mater. Des. 31, 1231-1236.

Elrefaey, A., Takahashi, M., Ikeuchi, K., 2004. Microstructure of Aluminum/Copper Lap Joint by Friction Stir Welding and its Performance. J. High Temp. Soc. 30, 286-292.

Firouzdor, V., Kou, S., 2012. Al-to-Cu Friction Stir Lap Welding. Metall. Mater. Trans. A 43A, 303-315.

Galvão, I., Leal, R.M., Rodrigues, D.M., Loureiro, A., 2013. Influence of tool shoulder geometry on properties of friction stir welds in thin copper sheets. J. Mater. Process. Technol. 213, 129-135.

Galvão, I., Oliveira, J.C., Loureiro, A., Rodrigues, D.M., 2011. Formation and distribution of brittle structures in friction stir welding of aluminium and copper: influence of process parameters. Sci. Technol. Weld. Joining 16, 681-689.

Galvão, I., Oliveira, J.C., Loureiro, A., Rodrigues, D.M., 2012. Formation and distribution of brittle structures in friction stir welding of aluminium and copper: Influence of shoulder geometry. Intermetallics 22, 122-128.

Hirata, T., Oguri, T., Hagino, H., Tanaka, T., Chung, S.W., Takigawa, Y., Higashi, K., 2007. Influence of friction stir welding parameters on grain size and formability in 5083 aluminum alloy. Mater. Sci. Eng. A 456, 344-349.

Humphreys, F.J., 2004. Characterisation of fine-scale microstructures by electron backscatter diffraction (EBSD). Scr. Mater. 51, 771-776.

Leitão, C., Loureiro, A., Rodrigues, D.M., 2011. Influence of Base Material Properties and Process Parameters on Defect Formation during FSW. In: Koçak, M. (Eds.), Proceedings of International Congress on Advances in Welding Science and Technology for Construction, Energy & Transportation Systems, Antalya, Turkey, pp. 177-184.

Leitão, C., Louro, R., Rodrigues, D.M., 2012. Analysis of high temperature plastic behaviour and its relation with weldability in friction stir welding for aluminium alloys AA5083-H111 and AA6082-T6. Mater. Des. 37, 402-409.

Leitão, C., Louro, R., Rodrigues, D.M., 2012. Using torque sensitivity analysis in accessing Friction Stir Welding/Processing conditions. J. Mater. Process. Technol. 212, 2051-2057.

Ma, Z.Y., Mishra, R.S., 2005. Development of ultrafine-grained microstructure and low temperature (0.48 Tm) superplasticity in friction stir processed Al-Mg-Zr. Scr. Mater. 53, 75-80.

Maitland, T., Sitzman, S., 2007. Electron Backscatter Diffraction (EBSD) Technique and Materials Characterization Examples. In: Zhou, W., Wang, Z.L. (Eds.), Scanning Microscopy for Nanotechnology, Springer, New York, pp. 41-75.

Ouyang, J., Yarrapareddy, E., Kovacevic, R., 2006. Microstructural evolution in the friction stir welded 6061 aluminum alloy (T6-temper condition) to copper. J. Mater. Process. Technol. 172, 110-122.

Saeid, T., Abdollah-Zadeh, A., Sazgari, B., 2010. Weldability and mechanical properties of dissimilar aluminum - copper lap joints made by friction stir welding. J. Alloys Compd. 490, 652-655.

Sato, Y.S., Urata, M., Kokawa, H., Ikeda, K., 2003. Hall-Petch relationship in friction stir welds of equal channel angular-pressed aluminium alloys. Mater. Sci. Eng. A 354, 298-305.

Svensson, L.E., Karlsson, L., Larsson, H., Karlsson, B., Fazzini, M., Karlsson, J., 2000. Microstructure and mechanical properties of friction stir welded aluminium alloys with special reference to AA 5083 and AA 6082. Sci. Technol. Weld. Joining 5, 285-96.

Topping, T.D., Ahn, B., Li, Y., Nutt, S.R., Lavernia, E.J., 2012. Influence of Process Parameters on the Mechanical Behavior of an Ultrafine-Grained Al Alloy. Metall. Mater. Trans. A 43, 505-519.

Tronci, A., McKenzie, R., Leal, R.M., Rodrigues, D.M., 2011. Microstructural and mechanical characterisation of 5XXX-H111 friction stir welded tailored blanks. Sci. Technol. Weld. Joining 16, 433-439.

Xue, P., Ni, D.R., Wang, D., Xiao, B.L., Ma, Z.Y., 2011. Achieving high property friction stir welded aluminium/copper lap joint at low heat input. Sci. Technol. Weld. Joining 16, 657-661.

Youssef, K.M., Scattergood, R.O., Murty, K.L., Koch, C.C., 2006. Nanocrystalline Al-Mg alloy with ultrahigh strength and good ductility. Scr. Mater. 54, 251-256.

FIGURE CAPTIONS

Figure 1 - Schematic representation of Al/Cu friction stir welding.

Figure 2 - Friction stir welding tool.

Figure 3 - Surface photograph (a); copper (b) and aluminium (c) etched cross-section macrographs and micrograph of the aluminium stirred zone (d) of the W5 weld.

Figure 4 - Surface photograph (a); copper (b) and aluminium (c) etched cross-section macrographs and micrographs of the under shoulder copper structure (d) and of the mixing structures (e) of the W6 weld.

Figure 5 - Hardness profiles registered across the transverse cross-section of the W5 (a) and W6 (b) welds.

Figure 6 - Hardness values registered in the aluminium stirred region of the W5 weld, in the vicinity of the Al-Cu interface.

Figure 7 - Results of the XRD inspection carried out in the stirred zone of the W5 (a) and W6 (b) welds.

Figure 8 - Qualitative chemical analysis (EPMA) carried out in the stirred aluminium region of the W5 weld, in the vicinity of the Al-Cu interface.

Figure 9 - TEM micrograph registered in the stirred aluminium region of the W5 weld (a) and the grain size distribution in that zone (b).

Figure 10 - EBSD patterns acquired in the stirred aluminium layer of the W5 weld, in the vicinity of the Al-Cu interface (a), and in the AA 5083 base material (b).

Figure 11 - Hall-Petch relationship for ultra-fine grained AA 5083 aluminium alloy.

HIGHLIGHTS

Aluminium nature had strong influence on Al/Cu friction stir lap welding results;

Strong materials interaction took place during AA 6082/copper friction stir welding;

No materials interaction took place during AA 5083/copper friction stir welding;

Hard and refined microstructures were formed in the AA 5083/copper welds;

Tool geometry/dimensions were decisive in microstructural evolution during welding.